Simple and versatile long range swept source for optical coherence tomography applications

2015 J. Opt. 17 125301

(http://iopscience.iop.org/2040-8986/17/12/125301)

OPEN ACCESS
IOP Publishing
Journal of Optics
J. Opt. 17 (2015) 125301 (5pp)
doi:10.1088/2040-8978/17/12/125301

Simple and versatile long range swept source for optical coherence tomography applications

Bastian Bräuer, Norman Lippok, Stuart G Murdoch and Frédérique Vanholsbeeck

The Dodd-Walls Centre for Photonic and Quantum Technologies, The Department of Physics, The University of Auckland, 38 Princes Street, Auckland, New Zealand

E-mail: bbra870@aucklanduni.ac.nz

Received 20 July 2015, revised 16 September 2015
Accepted for publication 17 September 2015
Published 27 October 2015

Abstract

We present a versatile long coherence length swept-source laser design for optical coherence tomography applications. This design consists of a polygonal spinning mirror and an optical gain chip in a modified Littman–Metcalf cavity. A narrowband intra-cavity filter is implemented through multiple passes off a diffraction grating set at grazing incidence. The key advantage of this design is that it can be readily adapted to any wavelength regions for which broadband gain chips are available. We demonstrate this by implementing sources at 1650 nm, 1550 nm, 1310 nm and 1050 nm. In particular, we present a 1310 nm swept source laser with 24 mm coherence length, 95 nm optical bandwidth, 2 kHz maximum sweep frequency and 7.5 mW average output power. These parameters make it a suitable source for the imaging of biological samples.

Keywords: long coherence length, optical coherence tomography, swept-source

(Some figures may appear in colour only in the online journal)

1. Introduction

Optical coherence tomography (OCT) is a real time, non-invasive and non-contact imaging modality for translucent and transparent tissue at micron scale resolution. First developed in 1991 [1], OCT became a favored technique for imaging the human eye because of its imaging capabilities, even in the early 1990s [2, 3]. Today, OCT is used to image a wide variety of tissues and non-biological structures [4–7]. Swept-source OCT, or optical frequency domain imaging (OFDI), has proven to be superior over time-domain OCT in terms of imaging speed and sensitivity [8–10]. The increase in imaging speed makes OFDI the better choice for real time imaging. Early swept sources used resonant galvanometers and polygon-scanners to implement the required intra-cavity wavelength-scanning filter. Polygon mirror based swept sources are easy to built with off the shelf components and their linear sweep and low cost make them a good solution for swept source configurations despite of their bulky appearance. At present a 10 facet slow scanning mirror cost about 2 000 USD while a fast scanning 72 facet mirror is 6 000 USD. Fourier-domain mode-locked lasers (FDML) based around Fabry–Perot (FP) tunable filters have played a prominent role in more recent designs [10, 11]. Fabry–Perot tunable filters achieve >100 kHz sweep rate, their disadvantage however is the highly nonlinear sweep, temperature drift and instability low-coherence length at low power [12–14]. Numerous companies have now transferred bulk and fiber-based schemes into commercial lasers that use MEMS mirrors or fast scanning FP to implement the intra-cavity filter and achieve the performance specifications required for high quality, high speed imaging for example (Optores GmbH,

Exalos AG, Santec Co., Axsun Inc., Praevium). However, such sources are still expensive and customizing their performance and specifications is difficult. MEMS based swept sources are manufactured by means of lithography and changing the center wavelength and bandwidth means changing the whole design process of the chip and buying a whole new source (currently around 30 000 USD).

Comparing these systems, polygon scanning mirrors are the cheapest and most flexible option to build fast and versatile sources and, for laboratories which do not have the capability to manufacture MEMS based systems, they are a good choice. MEMS based systems are, however, likely to go down in price if built in high volumes.

Apart from output power and scanning speed, clinical applications such as the measurement of the anterior segment of the eye, intravascular, gastrointestinal as well ontological diagnoses require long ranging depths and thus a superior coherence length. Several reports have demonstrated increased coherence length sources [15–17]. Two of the most recent technologies are multi-section 'akinetic' DBR lasers [18] and MEMS based VCSELS [16]. Both these designs allowing for narrow linewidths at very high sweep rates. However, to date the majority of these new sources operate around 1500 nm, a wavelength that is not suitable to image samples with high water absorption.

In summary, the need for swept sources which are reconfigurable to fit the needs of the application and are inexpensive still remains [19]. In this manuscript, we describe a filter and laser design that meets these objectives with an enhanced focus on improved coherence length, i.e. ranging depth. We present a new and simple swept source that is based on a modified Littman–Metcalf cavity. The design possesses a long coherence length and is extremely flexible as it uses standard free-space optical components and can be easily adapted to any wavelength region where semiconductor laser gain chips are available. With off-the-shelf optical components, this cavity can be quickly built with versatile performance and specification requirements at center wavelengths between 1 μm and 1.7 μm.

2. Method

The proposed cavity is based on the Littman–Metcalf configuration [20] as depicted in figure 1. The design is widely used in the telecommunications industry and is known to yield narrow instantaneous linewidths over a wide tuning range [21]. The laser diodes used in this experiment are commercially available single angled facet gain chips (Thorlabs). Their center wavelengths are 1050 nm, 1310 nm, 1550 nm and 1650 nm. The cavity for each source consists of a semiconductor gain chip, collimating optics, a diffraction grating, a gold coated polygonal mirror and an additional stationary mirror for the 1310 nm source and 1550 nm source. To achieve different center wavelengths, the gain chip is changed as well as the grating to be optimized for the new wavelength. The following explains the design of the 1310 nm cavity in detail as an example. The AR coated aspheric collimating lens has a focal length of 6.24 mm and gives a collimated beam diameter of 6 mm. The diffraction

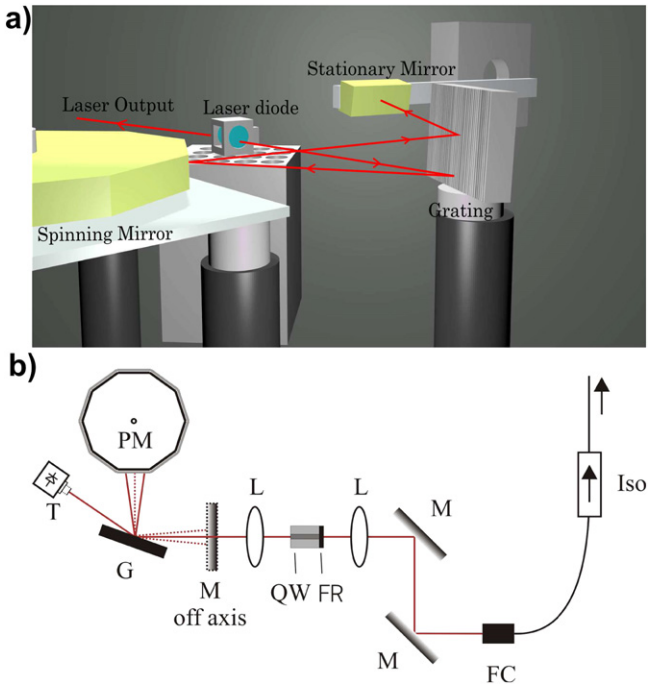

Figure 1. (a) Close up sketch of the cavity design for multiple illumination of the grating. The grating as well as the stationary mirror is on a tilt for alignment purposes. (b) Sketch of the swept source laser with the quantum well laser diode (QW), 10% facet reflection (FR), grating (G), mirror (M), lens (L), polygon mirror (PM), trigger (T), fiber collimator (FC) and isolator (Iso).

grating has 1200 lines mm^{-1} and is mounted at a grazing angle of 75 degrees with respect to the optical axis of the incoming beam. After the grating, the zeroth order output is detected by a photodiode to provide an electronic trigger, while the first order is reflected on to the polygonal mirror (Lincoln laser, DT-10-245-025). The mirror is a gold coated air bearing mirror with a velocity stability of 0.02%. Furthermore, the polygonal mirror has 10 facets, each with a width of 20 mm and a height of 6 mm, and can rotate between 6k and 24k rpm, giving a maximum sweep frequency of 4 kHz.

The cavity design uses a quadruple pass of the grazing incidence grating to achieve a very narrow intra-cavity filter resulting in good instantaneous linewidth. Further improvements to the linewidth can be made by additional passes through the grating, but this comes at the expense of increased intracavity loss and lower lasing power. To achieve this, the grating is slightly tilted and illuminates the spinning mirror at a vertical angle to obtain a vertical angular displacement between the incoming beam and reflected beam. The reflected beam is then retro reflected by a second stationary gold mirror placed after the diffraction grating to complete the cavity. The light exiting the laser cavity through the output facet with 10% reflectivity is collimated by an AR coated collimator ($f = 1.4$ mm) and is directed through a −55 dB optical isolator to prevent optical feedback into the laser cavity. For proof of concept imaging, the output of the swept source was directed to a Mach–Zehnder interferometer comprising a reference and sample arm. At the interferometer output, the mutual spectral density function of the interferometric signal was detected using a 100 MHz balanced photodetector. An Alazar Tech

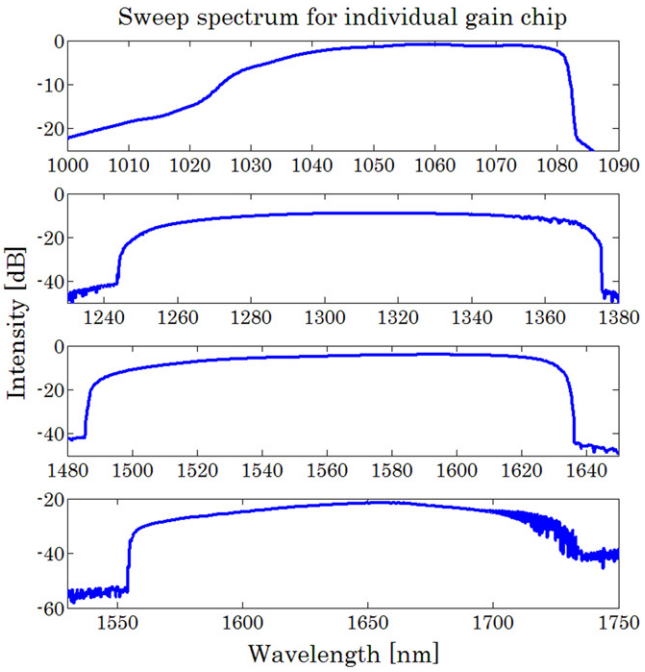

Figure 2. Spectral measurements of the sweep spectrum for the individual laser sources centered at 1050 nm, 1310 nm, 1550 nm and 1650 nm from top to bottom.

data acquisition card sampled the interference fringes at 125 MHz. To equally sample the interference fringes in *k*-space, a reference scan was taken prior to imaging. This linearization vector was used for resampling the interference spectrum for each consecutive A-scan. The linearization remained stable for more than 24 h. Zero padding was performed to increase digital resolution. Dispersion compensation was performed by inserting 1.3 mm of BK7 glass into the reference arm, after which the theoretical width of the point spread functions (PSF) was recovered [22, 23].

3. Results

Figure 2 shows the optical spectra for the four gain chips at a sweeping rate of 2 kHz. The OSA measurements show a 3 dB bandwidth of $\Delta\lambda_{1050} = 45$ nm, $\Delta\lambda_{1310} = 95$ nm, $\Delta\lambda_{1550} = 107$ nm and $\Delta\lambda_{1650} = 93$ nm. The inverse Fourier transform of the mutual spectral density yields the correlation function, which offered PSF of 13.4 μm, 10.3 μm, 12.6 μm and 12.6 μm respectively.

Coherence length measurements were performed using a basic fiber-based Mach–Zehnder interferometer as described above for the $\lambda_0 = 1310$ nm and $\lambda_0 = 1550$ nm source. The intensity of the coherence peak was measured as a function of path length difference. A 6 dB fall-off is observed at 12 mm, giving a total coherence length of 24 mm as shown in figure 3. The green curve indicates the depth range of a 6 dB fall-off. This result is comparable to commercially available sources but at a fraction of the cost. It is worth mentioning that we have also investigated the use of a second stationary mirror in the cavity, so as to obtain six passes off the diffraction grating. This resulted in a coherence length of

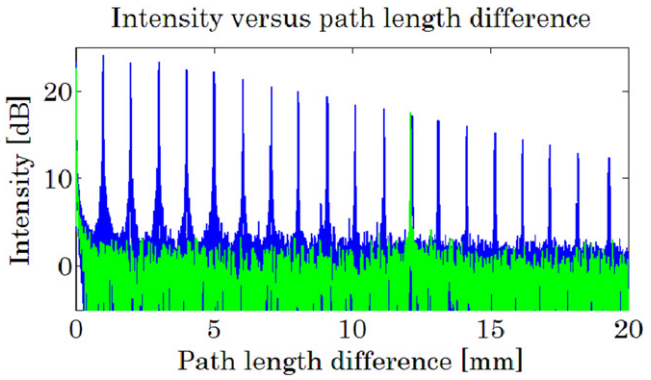

Figure 3. 6 dB intensity fall off at 12 mm path difference for the coherence length measurements indicated in green for the 1310 nm swept source.

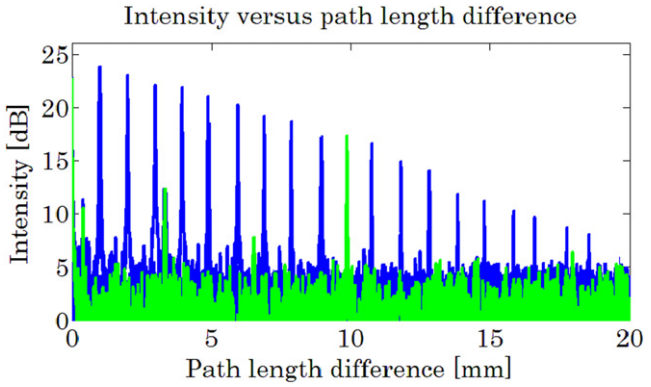

Figure 4. 6 dB intensity fall off at 10 mm path difference for the coherence length measurements indicated in green for the 1550 nm swept source.

30 mm, though at the expense of increased intra-cavity loss and lower output power. The power incident at the sample was 3.5 mW. To quantify the system sensitivity, a 30 dB neutral density filter was inserted into the sample arm. The sensitivity of the setup was measured to be 97 dB, making the source ideally suited for OCT imaging. To demonstrate the flexibility of the proposed design, we repeated these measurements for a cavity configuration using a gain chip centered at 1550 nm and a grating with 900 lines mm^{-1}. Coherence length measurements showed a 6 dB drop in intensity at a path difference of 10 mm in air, which resulted in a coherence length of 20 mm as shown in figure 4.

We calculated the effective laser linewidth using the measured coherence length, $l_c = 24$ mm, and equation (1) below [24]

$$\Delta\lambda_{\mathrm{FWHM}} = \frac{0.44 * (\lambda_0)^2}{l_c}. \quad (1)$$

We obtained a value of approximately 30 pm. To further characterize the performance of the swept source, an ocular length measurement of a sheep's eye and a depth measurement with a Perspex cube was performed. The Perspex cube was 40 × 40 × 30 mm^3 in size and had 14 boreholes, spread

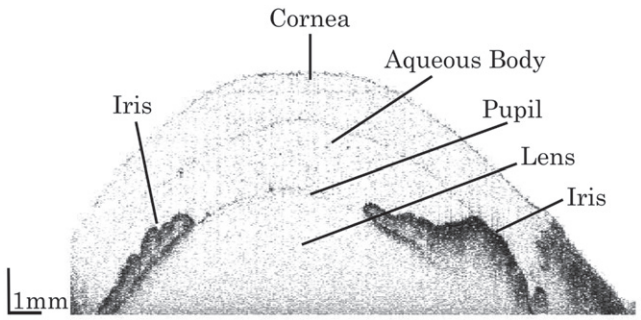

Figure 5. Image of a sheep eye with the anatomical correct parts, the cornea seems to be flat on top due to the loss of stiffness since the eye was taken out, stored and streched for imaging.

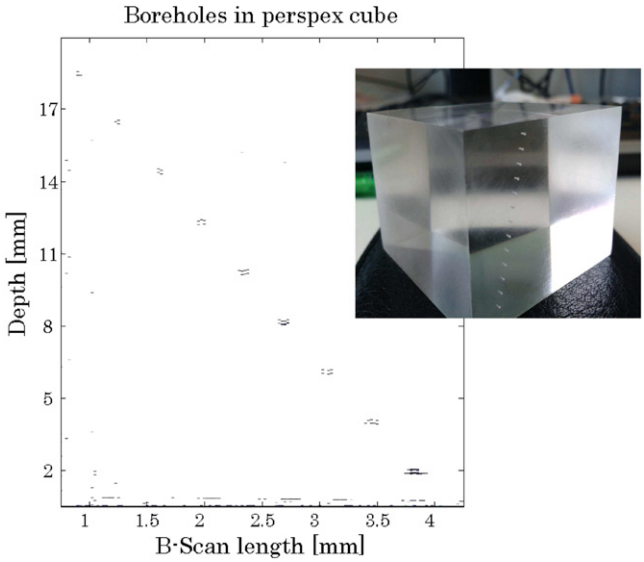

Figure 6. Depth measurements of a Perspex cube. The holes in the Perspex cube are 2 mm apart in depth and 500 μm in distance from each other. The ninth hole is the last hole to be identified as a structure which corresponds to 18 mm in depth from the zero path (bottom of cube).

vertical in 2 mm steps and horizontally in 0.5 mm steps. The holes had a diameter of roughly 300 μm and were laser drilled to a depth of 2 mm. Figure 5 shows a 15 mm cross section of the sheeps eye using the 1310 nm source. The anatomical parts of the eye such as the cornea, the aqueous body, the lens, the pupil and the iris can be clearly identified [25]. The depth resolution in the image is 12 μm which is higher than the theoretical PSF of the system and comes from a dispersion imbalance in the two interferometer arms. The lateral resolution is 25 μm. As a note, no averaging or filtering was performed on the image after aquisition. Figure 6 shows a photograph of the Perspex cube (inset) and the OCT image of the boreholes. Calculations from the measurements indicated borehole dimensions of 380 μm wide by 360 μm deep. The clearly resolved structures, separated by over 18 mm in depth, are a testimony of the long coherence length of the source.

4. Discussion

The presented results are comparable to commercially available sources at lower scan rates. We note that several groups have achieved higher scan speeds than 2 kHz with similar intra-cavity filter designs [26–28]. However the coherence length achieved in these systems (2–7 mm) is considerably lower than what is achieved here. The approach by Chong *et al* in a telescope less configuration achieved higher scan rates and longer coherence length at the expense of a significantly decreased bandwidth [29]. It is worth noticing that the demonstrated scanning speed of 2 kHz can be significantly increased. Indeed, a seven times increase in the number of mirror facets, as is typically used in standard polygon mirror based swept sources [30], would lead to a seven fold increase in A-line rate, without sacrificing cavity roundtrips. Moreover, careful adjustment of the sweeping duty cycle to 50% or 25% would further allow us to double and quadruple the facet limited A-line rate by employing a 2-fold or 4-fold interleaving scheme [31]. It should also be noted that an increase in output power can readily be obtain through post-amplification using appropriate semiconductor optical amplifier (SOA) at the cavity output. This was avoided here for proof of concept demonstration, yet a typical SOA saturation output power of 17 dBm could offer up to 70 mW output power.

5. Conclusion

In conclusion we have demonstrated a simple design for a stable long coherence length swept source that uses only standard optical components and that can be easily adapted to a variety of center wavelengths. Key to the narrow linewidth operation of this source is the 4-pass intra-cavity narrowband filter. The coherence length of 24 mm is comparable to commercially available swept sources and we have demonstrated its viability by making OCT measurements of a sheep eye and a perspex target.

References

[1] Huang D *et al* 1991 Optical coherence tomography *Science* **254** 1178–81
[2] Hee M R *et al* 1995 Optical coherence tomography of the human retina *Arch. Ophthalmol.* **113** 325–32
[3] Chan A, Duker J S, Ko T H, Fujimoto J G and Schuman J S 2006 Normal macular thickness measurements in healthy eyes using stratus optical coherence tomography *Arch. Ophthalmol.* **124** 193–8
[4] Vakoc B J, Fukumura D, Jain R K and Bouma B E 2012 Cancer imaging by optical coherence tomography: preclinical progress and clinical potential *Nat. Rev. Cancer* **12** 363–8
[5] Kim K H, Pierce M C, Maguluri G, Park B H, Yoon S J, Lydon M, Sheridan R and de Boer J F 2012 *In vivo* imaging of human burn injuries with polarization-sensitive optical coherence tomography *J. Biomed. Opt.* **17** 066012

[6] Chen J *et al* 2005 Gold nanocages: bioconjugation and their potential use as optical imaging contrast agents *Nano Lett.* **5** 473–7
[7] Targowski P, Gora M and Wojtkowski M 2006 Optical coherence tomography for artwork diagnostics *Laser Chem.* 1–1 2006
[8] Leitgeb R, Hitzenberger C and Fercher A 2003 Performance of fourier domain versus time domain optical coherence tomography *Opt. Express* **11** 889–94
[9] Choma M, Sarunic M, Yang C and Izatt J 2003 Sensitivity advantage of swept source and fourier domain optical coherence tomography *Opt. Express* **11** 2183–9
[10] Yun S-H, Boudoux C, Tearney G J and Bouma B E 2003 High-speed wavelength-swept semiconductor laser with a polygon-scanner-based wavelength filter *Opt. Lett.* **28** 1981–3
[11] Oh W-Y, Yun S H, Tearney G J and Bouma B E 2005 115 khz tuning repetition rate ultrahigh-speed wavelength-swept semiconductor laser *Opt. Lett.* **30** 3159–61
[12] Duma V-F and Podoleanu A G Polygon mirror scanners in biomedical imaging: a review *SPIE OPTO* (International Society for Optics and Photonics) 86210V
[13] Duma V-F, Rolland J P and Podoleanu A G Perspectives of optical scanning in OCT *BiOS* (International Society for Optics and Photonics) 75560B
[14] Huber R, Wojtkowski M, Taira K, Fujimoto J and Hsu K 2005 Amplified, frequency swept lasers for frequency domain reflectometry and OCT imaging: design and scaling principles *Opt. Express* **13** 3513–28
[15] Zabihian B, Minneman M, Bonesi M, Ensher J, Sattmann H, Gray S, Leitgeb R, Crawford M and Drexler W Akinetic swept-source technology for high speed OCT with unprecedented coherence length *Bio-Optics: Design and Application* (Optical Society of America) BT3A-2
[16] Potsaid B, Jayaraman V, Fujimoto J G, Jiang J, Heim P J and Cable A E MEMS tunable VCSEL light source for ultrahigh speed 60 kHz–1 mHz axial scan rate and long range centimeter class OCT imaging *SPIE BiOS* (International Society for Optics and Photonics) 82130M
[17] Chong C, Suzuki T, Totsuka K, Morosawa A and Sakai T 2009 Large coherence length swept source for axial length measurement of the eye *Appl. Opt.* **48** 144–50
[18] Minneman M P, Ensher J, Crawford M and Derickson D All-semiconductor high-speed akinetic swept-source for OCT *Communications and Photonics Conf. and Exhibition* (ACP. Asia, IEEE) pp 1–10
[19] Jun C, Villiger M, Oh W -Y and Bouma B E 2014 All-fiber wavelength swept ring laser based on Fabry–Perot filter for optical frequency domain imaging *Opt. Express* **22** 25805–14
[20] Littman M G and Metcalf H J 1978 Spectrally narrow pulsed dye laser without beam expander *Appl. Opt.* **17** 2224–7
[21] Duarte F J 1996 *Tunable Lasers Handbook* (New York: Academic)
[22] Wojtkowski M, Srinivasan V, Fujimoto T K J, Kowalczyk A and Duker J 2004 Ultrahigh-resolution, high-speed, fourier domain optical coherence tomography and methods for dispersion compensation *Opt. Express* **12** 2404–22
[23] Lippok N, Coen S, Nielsen P and Vanholsbeeck F 2012 Dispersion compensation in Fourier domain optical coherence tomography using the fractional fourier transform *Opt. Express* **20** 23398–413
[24] Wolfgang D and Fujimoto J G 2008 *Optical Coherence Tomography: Technology and Applications* (Berlin: Springer-Verlag)
[25] Fan S, Qin L, Dai C and Zhou C 2014 Dual illumination OCT at 1050 nm and 840 nm for whole eye segment imaging *SPIE/COS Photonics Asia* (International Society for Optics and Photonics) 92682O
[26] Leung M K K, Mariampillai A, Standish B A, Lee K K C, Munce N R, Vitkin I A and Yang V X D 2009 High-power wavelength-swept laser in littman telescope-less polygon filter and dual-amplifier configuration for multichannel optical coherence tomography *Opt. Lett.* **34** 2814–6
[27] Yun S, Tearney G, Johannes de Boer N, Iftimia and Bouma B 2003 High-speed optical frequency-domain imaging *Opt. Express* **11** 2953–63
[28] Motaghian Nezam S M R 2008 High-speed polygon-scanner-based wavelength-swept laser source in the telescope-less configurations with application in optical coherence tomography *Opt. Lett.* **33** 1741–3
[29] Chong C, Suzuki T, Morosawa A and Sakai T 2008 Spectral narrowing effect by quasi-phase continuous tuning in high-speed wavelength-swept light source *Opt. Express* **16** 21105–18
[30] Mao Y, Chang S, Murdock E and Flueraru C 2011 Simultaneous dual-wavelength-band common-path swept-source optical coherence tomography with single polygon mirror scanner *Opt. Lett.* **36** 1990–2
[31] Wieser W, Draxinger W, Klein T, Karpf S, Pfeiffer T and Huber R 2014 High definition live 3d-OCT *in vivo*: design and evaluation of a 4d OCT engine with 1 gvoxel s^{-1} *Biomed. Opt. Express* **5** 2963–77